

# Sparse linear modeling of next-generation mRNA sequencing (RNA-Seq) data for isoform discovery and abundance estimation

Jingyi Jessica Li (李婧翌)<sup>a</sup>, Ci-Ren Jiang<sup>b</sup>, James B. Brown<sup>a</sup>, Haiyan Huang<sup>a,1</sup>, and Peter J. Bickel<sup>a,1</sup>

<sup>a</sup>Department of Statistics, University of California, Berkeley, CA 94720; and <sup>b</sup>Statistical and Applied Mathematical Sciences Institute, Research Triangle Park, NC 27709-4006

Contributed by Peter J. Bickel, September 25, 2011 (sent for review June 22, 2011)

Since the inception of next-generation mRNA sequencing (RNA-Seq) technology, various attempts have been made to utilize RNA-Seq data in assembling full-length mRNA isoforms de novo and estimating abundance of isoforms. However, for genes with more than a few exons, the problem tends to be challenging and often involves identifiability issues in statistical modeling. We have developed a statistical method called “sparse linear modeling of RNA-Seq data for isoform discovery and abundance estimation” (SLIDE) that takes exon boundaries and RNA-Seq data as input to discern the set of mRNA isoforms that are most likely to present in an RNA-Seq sample. SLIDE is based on a linear model with a design matrix that models the sampling probability of RNA-Seq reads from different mRNA isoforms. To tackle the model unidentifiability issue, SLIDE uses a modified Lasso procedure for parameter estimation. Compared with deterministic isoform assembly algorithms (e.g., Cufflinks), SLIDE considers the stochastic aspects of RNA-Seq reads in exons from different isoforms and thus has increased power in detecting more novel isoforms. Another advantage of SLIDE is its flexibility of incorporating other transcriptomic data such as RACE, CAGE, and EST into its model to further increase isoform discovery accuracy. SLIDE can also work downstream of other RNA-Seq assembly algorithms to integrate newly discovered genes and exons. Besides isoform discovery, SLIDE sequentially uses the same linear model to estimate the abundance of discovered isoforms. Simulation and real data studies show that SLIDE performs as well as or better than major competitors in both isoform discovery and abundance estimation. The SLIDE software package is available at <https://sites.google.com/site/jingyijli/SLIDE.zip>.

mRNA isoform discovery | single-end vs. paired-end sequencing | fragment length distribution | GC contents | penalized estimation

The recently developed next-generation mRNA sequencing (RNA-Seq) assay, with deep coverage and base level resolution, has provided a view of eukaryotic transcriptomes of unprecedented detail and clarity. Unlike microarrays, RNA-Seq data have novel splice junction information in addition to gene expression, thus facilitating whole-transcriptome assembly and mRNA isoform quantification. RNA-Seq data includes both single-end and paired-end reads, where a single-end read is a sequenced end of a cDNA fragment from an mRNA transcript, and a paired-end read is a mate pair corresponding to both ends of a cDNA fragment.

In the mRNA isoform discovery field, one of the most widely used software packages is Cufflinks (1). It builds a set of genes and exons solely from RNA-Seq data first, and subsequently uses a deterministic approach to find a minimal set of isoforms that can explain all the cDNA fragments indicated by paired-end reads. Cufflinks mainly uses qualitative exon expression and junction information in its isoform discovery, lacking a quantitative consideration of RNA-Seq data. Although Cufflinks gives very useful results, we note that the isoforms it discovers based on de novo assembled genes and exons can be heavily biased by differ-

ent types of RNA-Seq data noise (2–5). Two recently published modENCODE (Model Organism Encyclopedia of DNA Elements) (6) consortium papers (7, 8) also raise concerns about relying solely on RNA-Seq reads in isoform discovery and have suggested using manual annotations to scrutinize the results.

In the mRNA isoform quantification field, the question is to estimate the abundance of isoforms in a given set. Available abundance estimation methods include direct computation (9, 10) and model-based approaches. Many model-based studies (1, 11–14) have used maximum-likelihood approaches to estimate isoform abundance. There are also efforts on formulating the abundance estimation problem as a linear model (15), where the independent and dependent variables are isoform expression levels and categorized RNA-Seq read counts, respectively. In particular, binary values have been used in the design matrix to relate categorized reads to different isoforms, but that design matrix misses the quantitative relationship between read quantities and isoform abundance.

In this study, we propose a statistical method called “sparse linear modeling of RNA-Seq data for isoform discovery and abundance estimation” (SLIDE) that uses RNA-Seq data to discover mRNA isoforms given an extant annotation of gene and exon boundaries, and to estimate the abundance of the discovered or other specified mRNA isoforms. The extant annotation can come from annotation databases [e.g., Ensembl (16) or UCSC Genome Browser (17)], can be supplemented by other transcriptomic data such as RACE or CAGE (18, 19), or can even be inferred from RNA-seq de novo assembly algorithms (1, 20). SLIDE is based on a linear model with a nonbinary design matrix modeling the sampling probability of RNA-Seq reads from mRNA isoforms. When modeling the design matrix, we considered the effects of GC content, cDNA fragment lengths, and read starting positions. This linear model, coupled with the carefully defined design matrix, gives SLIDE a stochastic property of making use of exon expression quantitatively in isoform discovery. The SLIDE model can also be easily extended to incorporate other transcriptomic data [e.g., RACE (18), CAGE (19), and EST (21)] with RNA-Seq to achieve more comprehensive results. The SLIDE software package is available at <https://sites.google.com/site/jingyijli/SLIDE.zip>.

Author contributions: J.J.L., C.-R.J., H.H., and P.J.B. designed research; J.J.L., C.-R.J., and H.H. performed research; J.J.L. and C.-R.J. contributed new reagents/analytic tools; J.J.L., C.-R.J., and H.H. analyzed data; and J.J.L., J.B.B., H.H., and P.J.B. wrote the paper. The authors declare no conflict of interest.

Data deposition: The sequences reported in this paper have been deposited in the Sequence Read Archive, <http://www.ncbi.nlm.nih.gov/sra> (accession nos. SRX003838, SRX003839, SRX003836, SRX003837, SRR070261, SRR070269, SRR111873, SRR023600, SRR035402, SRR023720, SRR023715, SRR023751, SRR023707, and SRR023826).

<sup>1</sup>To whom correspondence may be addressed. E-mail: [bickel@stat.berkeley.edu](mailto:bickel@stat.berkeley.edu) or [hhuang@stat.berkeley.edu](mailto:hhuang@stat.berkeley.edu).

This article contains supporting information online at [www.pnas.org/lookup/suppl/doi:10.1073/pnas.1113972108/-DCSupplemental](http://www.pnas.org/lookup/suppl/doi:10.1073/pnas.1113972108/-DCSupplemental).

## Results

**Linear Modeling for RNA-Seq Data.** SLIDE is designed as a tool for discovering mRNA isoforms and estimating isoform abundance from RNA-Seq reads, on top of known information about gene and exon boundaries. For isoform discovery, SLIDE considers all the possible isoforms by enumerating exons of every gene. For example, a gene of  $n$  nonoverlapping exons has  $2^n - 1$  possible isoforms, each composed of a subset of the  $n$  exons. However, because of the possible occurrence of alternative splicing within exons, isoforms of the same gene may have partially overlapping but different exons. Hence, for ease of enumeration, we define a subexon as a transcribed region between adjacent splicing sites in any annotated mRNA isoforms (Fig. 1A). With this definition, every gene has a set of nonoverlapping subexons, from which we can enumerate all the possible isoforms including annotated ones.

We formulate the task of discovering isoforms for a given gene as a sparse estimation problem where the sparseness applies to the isoforms expected from RNA-Seq data. Because exon expression levels and the existence of possible exon–exon junctions are the key for isoform discovery and they can be inferred from the starting and ending positions of RNA-Seq reads mapped to a reference genome, we are motivated to transform RNA-Seq reads into a summary that captures the key information. For a paired-end read, we exact four genomic locations  $s_1, e_1, s_2,$  and  $e_2$ , where  $s_1$  and  $e_1$  are the starting and ending positions of its 5' end, and  $s_2$  and  $e_2$  are the starting and ending positions of its 3' end (Fig. 1B). Note that a paired-end read uniquely corresponds to a cDNA fragment with both ends sequenced, that is,  $s_1$  and  $e_2$  are the starting and ending positions of the fragment, respectively. We next categorize paired-end reads into paired-end bins defined as four-dimensional vectors: Bin  $(i, j, k, l)$  contains reads whose  $s_1, e_1, s_2,$  and  $e_2$  are in subexons  $i, j, k,$  and  $l$ , respectively (see *Methods* for details). For single-end reads, we can similarly categorize them into two-dimensional single-end bins. The so-defined bin counts provide all the exon expression and junction information.

SLIDE is built upon a linear model whose design matrix  $\mathbf{F}$  models conditional probabilities of observing reads in different bins given an isoform. For paired-end data, modeling  $\mathbf{F}$  requires distributional assumptions on the two ends (i.e.,  $s_1, e_2$ ) of a cDNA fragment in an mRNA transcript, or equivalently on the fragment's 5' end (i.e.,  $s_1$ ) and its length (i.e.,  $e_2 - s_1$ ). For  $s_1$ , uniform distribution assumptions have been widely used. However, after considering the high correlation observed between sequencing read coverage and genome GC content (2), we assume the density of  $s_1$  is uniform within subexons and proportional to the GC content between subexons. We specify the distribution of the fragment length,  $e_2 - s_1$ , by assuming  $e_2$  to follow a Poisson point process given  $s_1$  fixed. Consequently,  $e_2 - s_1$  is modeled as truncated Exponential after taking into account the size selection step in RNA-Seq protocols (see *Methods*). Another widely used fragment length distribution is Normal distribution (1), which is also implemented in SLIDE and compared with truncated Exponential (see *SI Text*).

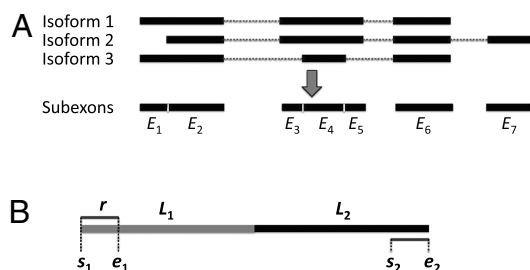


**Fig. 1.** (A) Definition of subexons: transcribed regions between adjacent alternative splicing sites. (B) A two-exon mRNA transcript.  $s_1, e_1, s_2,$  and  $e_2$ , genomic positions associated with a paired-end read.  $r$ , the read end length;  $L_1$  and  $L_2$ , the exon lengths.

We then use a linear model as approximation to the observed bin proportions,

$$b_j = \sum_{k=1}^K F_{jk} p_k + \epsilon_j, \quad j = 1, \dots, J, \quad [1]$$

where  $b_j$  is the observed proportion of reads in the  $j$ th bin,  $F_{jk} = \Pr(j\text{th bin}|k\text{th isoform})$  (i.e., the conditional probability of observing paired-end reads in the  $j$ th bin given that they are from the  $k$ th isoform),  $p_k$  is the proportion of the  $k$ th isoform to be estimated, and  $\epsilon_j$  is the error term with mean 0. Besides,  $J$  and  $K$  are the numbers of bins and isoforms, respectively (see *Methods*). This is the core linear model used in SLIDE for both isoform discovery and abundance estimation of discovered isoforms. For isoform discovery, usually  $K > J$ , so the model is unidentifiable. But based on biological knowledge, we expect the model to be sparse and achieve sparse estimation by a modified Lasso (22) method (see *Methods*). For abundance estimation, only the proportions of discovered isoforms are parameters in the linear model, and their number is often far less than  $K$ , so there is no identifiability issue anymore. SLIDE then does the parameter estimation by nonnegative least squares. Compared with maximum-likelihood approaches used by other abundance estimation methods, SLIDE has the computational advantage of fitting a linear model as an intrinsic element.

**Simulation Results.** A simulation study is used to assess the accuracy of SLIDE on isoform discovery and abundance estimation. We simulated reads from genes and true mRNA isoforms extracted from *Drosophila melanogaster* annotation (September 2010) of UCSC Genome Browser (17). For illustration purposes, we focus on the 3,421 genes on chr3R. Based on our defined subexons, those genes consist of 34.2% with 1–2 subexons, 57.6% with 3–10 subexons, and 8.2% with more than 10 subexons. Because the estimation for genes with 1–2 subexons is trivial due to their small numbers of possible isoforms, and genes with more than 10 subexons only constitute a small proportion and their estimation is computationally costly, we applied SLIDE to the subset of 3–10 subexons, 1,972 genes in total. We generated  $500 \times 50$  (runs) paired-end reads for each gene from annotated isoforms of randomly defined proportions, and then we applied SLIDE to the simulated reads for isoform discovery and abundance estimation.

The isoform discovery results of all 50 runs are in Fig. 2A. We divided genes into groups by their numbers of subexons  $n$  ( $n = 3, \dots, 10$ ). For each gene, SLIDE returns a vector of estimated proportions of all its possible isoforms. We define isoforms whose estimated proportions exceed threshold 0.1 as discovered isoforms and evaluate them by the UCSC annotation. (Note that other thresholds 0.05 and 0.2 return similar results.) For each gene, the precision rate is defined as  $TP/(TP + FP)$ , and the recall rate is  $TP/(TP + FN)$ , where  $TP$  is the number of true positives (discovered isoforms that are also in the annotation),  $FP$  is the number of false positives (discovered isoforms that are not in the annotation), and  $FN$  is the number of false negatives (undiscovered isoforms that are in the annotation and have every exon observed). For each group of  $n$ -subexon genes, we calculated their average precision and recall rates as presented in Fig. 2A. The results show that SLIDE maintains high precision rates (>80%) and good recall rates (>60%) in all groups of genes. In particular, for genes with three and four subexons, the precision and recall rates are greater than 98% and 92%, respectively. As  $n$  increases, the precision and recall rates decrease, and the variance between different simulation runs increases. This observation is reasonable because with the increase of  $n$ , the number of possible isoforms increases exponentially, as does the difficulty of isoform discovery.

To illustrate the abundance estimation accuracy of SLIDE, we applied it to 317 multi-isoform genes on chr3R in the UCSC





**Table 1. modENCODE datasets used in the analysis**

Dataset	Type	Sample	Read length	Total number of reads	Sequence Read Archive ( <a href="http://www.ncbi.nlm.nih.gov/sra">http://www.ncbi.nlm.nih.gov/sra</a> ) numbers
1	paired-end	ML-DmBG3-c2	37 bp	25,094,224	SRX003838, SRX003839
2	paired-end	Kc167	37 bp	18,602,220	SRX003836, SRX003837
3	paired-end	Kc167	76 bp	20,118,748	SRR070261, SRR070269, SRR111873
4	paired-end and single-end	embryo 16-17h	76 bp	23,388,810 and 27,913,445	SRR023600, SRR035402, SRR023720, SRR023715, SRR023751, SRR023707, SRR023826

By a detailed inspection of the isoforms discovered by Cufflinks, we find that many discovered isoforms are fragments of annotated isoforms in public databases. This is mainly due to the difficulty in de novo construction of gene boundaries. Cufflinks also has troubles in detecting lowly expressed genes de novo. By contrast, SLIDE can discover correct isoforms even with a small number of reads, based on existing gene boundary information. For instance, when applied to dataset 1, SLIDE has discovered isoforms in 1,084 genes (RPKM > 1) out of the total 1,972 genes, whereas Cufflinks has only found isoforms in 801 genes. These observations confirm again the importance of having correct gene boundaries in isoform discovery. Another advantage of SLIDE is the usage of a stochastic approach to simultaneously detect isoforms with alternative starts/ends [e.g., (1,2,3,4) and (2,3,4)], where Cufflinks will only discover the longest one (1). However, when there are significant RNA-Seq data biases in 5' and 3' ends of mRNA transcripts, the deterministic approach of Cufflinks may be more robust. In the future, with the continuing development of sequencing technology and promising improvement in RNA-Seq signal-to-noise ratios, we would expect the stochastic approach of SLIDE to be preferred.

There are other isoform discovery methods that use sparse estimation but with different methodology (15, 24). A numerical comparison between SLIDE and IsoLasso (15) shows that SLIDE has higher accuracy in isoform discovery. For detailed comparison information, please see *SI Text*.

**mRNA Isoform Abundance Estimation on modENCODE Data.** Another feature of SLIDE is to estimate the abundance of mRNA isoforms discovered or other specified (e.g., annotated) from an RNA-Seq sample. Because of the lack of ground truth of isoform abundance in datasets 1–4 (Table 1), to evaluate the abundance estimation performance of SLIDE, we compare its estimates to those of two popular methods: statistical inferences for isoform expression in RNA-Seq (SIER) (12) and Cufflinks (1). Note that SLIDE returns estimates of mRNA isoform proportions that are equivalent and convertible to the common abundance measure, isoform RPKMs (10) used in SIER.

In the comparison between SLIDE and SIER, both methods estimate the isoform abundance of the 317 chr3R genes with multiple isoforms in the UCSC annotation. In dataset 1, after removing 25 genes with high expression variance among exons (see *SI Text*), we obtain a scatter plot of the two sets of estimates in Fig. 3B ( $R = 0.88$ ). A similar comparison is carried out between SLIDE and Cufflinks, and the results are in Fig. 3C ( $R = 0.85$ ). The results show that SLIDE obtains estimates similar to those of SIER and Cufflinks. For more discussions on the results, see *SI Text*.

**Miscellaneous Effects on Isoform Discovery.** Using datasets 1–4 (Table 1), we study the following critical issues affecting isoform discovery from RNA-Seq data.

1. GC content variation. To study the usefulness of considering GC content variation in isoform discovery, we additionally implemented another version of **F**, assuming the cDNA fragment starting position  $s_1$  as uniform across all subexons. Note that our default **F** assumes the density of  $s_1$  as uniform within subexons but proportional to GC content between subexons, as motivated by observed high correlation between read coverage and GC content variation (2, 4) (see *SI Text*). Isoform discovery results on dataset 1 by SLIDE based on the two version of **F** are compared in Table 2. Recall rates are similar in both results, but precision rates are improved with the consideration of GC content. These results indicate that GC content can provide SLIDE with useful information in modeling **F**, and thus support various attempts of using GC content information to correct RNA-Seq data noise (3, 4).
2. Read/fragment length effects. To explore the effects of RNA-Seq read lengths on isoform discovery, we applied SLIDE to datasets 2 and 3. The two datasets are generated from the same Kc167 sample of similar sequencing depth but with different read lengths: 37 bp (dataset 2) vs. 76 bp (dataset 3). We compare the isoform discovery results on both datasets in Fig. 4A. The precision and recall rates for genes with 3–9 subexons are surprisingly higher with the 37-bp data than the 76-bp data. This result contradicts our expectation that RNA-Seq data with longer read length would provide more information on exon junctions that are crucial to isoform discovery. Trying to find a plausible explanation, we checked the empirical distribution of cDNA fragment lengths in single-exon genes for both data, and found the distribution close to  $N(166, 26^2)$  and  $N(127, 13^2)$  for the 37-bp and 76-bp data, respectively. The fact that the 37-bp data contain more long fragments is a result of different experimental protocols, and is likely to be a reason for the observed unexpected comparison results. A simulation study with different read and fragment lengths reveals that the fragment length distribution has larger effects than the read length has on isoform discovery, and to some extent confirms our real data observation (see *SI Text*).
3. Paired-end vs. single-end RNA-Seq data. Compared with single-end RNA-Seq data, the more recent paired-end data provides more information on exon junctions and thus is expected to return isoform discovery results with higher precision rates. But if both single-end and paired-end data are available for the same RNA-Seq sample, the former can possibly complement the latter by providing more exon expression information, helping capture lowly expressed exons in rare

**Table 2. Comparison of isoform discovery results by SLIDE with two versions of **F****

$n$		3	4	5	6	7	8	9	10
without GC	precision	0.93	0.90	0.87	0.80	0.83	0.75	0.71	0.49
	recall	0.91	0.89	0.83	0.77	0.71	0.68	0.61	0.36
with GC	precision	0.94	0.92	0.90	0.82	0.87	0.79	0.74	0.56
	recall	0.91	0.89	0.84	0.78	0.71	0.67	0.60	0.38



For single-end data and the combination of both single and paired-end data, we can derive a similar linear model (see *SI Text*).

**Modeling of Conditional Probability Matrix.** Modeling of the conditional probability matrix  $F = (F_{jk})$ ,  $1 \leq j \leq J$ ,  $1 \leq k \leq K$  is a key part in the estimation of  $\mathbf{p}$  (Eq. 3). In paired-end RNA-Seq data, a mate pair represents ends of a cDNA fragment reversely transcribed from an mRNA transcript. In this sense,  $F_{jk}$  is the conditional probability that cDNA fragments with ends in the  $j$ th bin are reversely transcribed from mRNA transcripts in the  $k$ th isoform. With this interpretation, we model  $F$  with the following three assumptions.

1. The density of a cDNA fragment's starting position (or the density of  $s_1$  in Fig. 1), denoted by  $f$ , is uniform within subexons but proportional to GC content between subexons in an mRNA transcript.
2. The cDNA fragment length ( $\ell = e_2 - s_1$  in Fig. 1) distribution is modeled as truncated Exponential with density denoted by  $g$ . This modeling choice is based on empirical observations and Poisson point process approximations (see *SI Text*). SLIDE can also easily take other reasonable fragment length distributions.
3. Starting positions and fragment lengths are assumed to be independent.

In a two-subexon gene example (Fig. 1), suppose that the two subexons have boundaries  $[a_1, b_1]$  and  $[a_2, b_2]$ . Then, reads in bin  $j = (1, 1, 2, 2)$  have  $s_1 \in [a_1, b_1 - r + 1]$  and  $e_2 \in [a_2 + r - 1, b_2]$ . For  $k = (1, 2)$ , we calculate  $F_{jk} = \int_{a_1}^{b_1 - r + 1} f(s_1) \int_{a_2 + r - 1}^{b_2} g(\ell) d\ell ds_1$ .

For single-end data and the combination of both single and paired-end data,  $F$  can be similarly calculated (see *SI Text*).

**mRNA Isoform Discovery.** In isoform discovery, we expect sparse parameter estimation from the linear model (Eq. 3), because the number of mRNA isoforms for most *D. melanogaster* genes is below four (17) and far less than the number of possible isoforms  $K$ .  $L_1$  penalization approach is widely used for sparse estimation and has applications in high-dimensional and potentially sparse biological data (25). We also observe that annotated isoforms often contain a large proportion of subexons, and thus expect isoform candidates with more subexons to be more likely true. Hence, we add an  $L_1$  penalty term in the objective function below to limit the number of discovered isoforms as well as to favor the "longer isoforms":

$$\hat{\mathbf{p}} = \operatorname{argmin}_{p_1, \dots, p_k \geq 0} \sum_{j=1}^J (b_j - \mathbf{F}_j \mathbf{p})^2 + \lambda \sum_{k=1}^K \frac{|p_k|}{n_k}, \quad [4]$$

where  $n_k$  is the number of subexons in the  $k$ th isoform and  $\mathbf{F}_j$  is the  $j$ th row of  $F$ . With  $n_k$  in the penalty term,  $p_k$  would thus be favored if  $n_k$  is large. We

1. Trapnell C, et al. (2010) Transcript assembly and quantification by RNA-Seq reveals unannotated transcripts and isoform switching during cell differentiation. *Nat Biotechnol* 28:511–515.
2. Dohm JC, Lottaz C, Borodina T, Himmelbauer H (2010) Substantial biases in ultra-short read data sets from high-throughput DNA sequencing. *Nucleic Acids Res* 36:e105.
3. Hansen KD, Brenner SE, Dudoit S (2010) Biases in Illumina transcriptome sequencing caused by random hexamer priming. *Nucleic Acids Res* 38:e131.
4. Li J, Jiang H, Wong WH (2010) Modeling non-uniformity in short-read rates in RNA-Seq data. *Genome Biol* 11:R50.
5. Roberts A, Trapnell C, Donaghey J, Rinn JL, Pachter L (2011) Improving RNA-Seq expression estimates by correcting for fragment bias. *Genome Biol* 12:R22.
6. modENCODE Consortium (2009) Unlocking the secrets of the genome. *Nature* 459:927–930.
7. modENCODE Consortium (2010) Identification of functional elements and regulatory circuits by *Drosophila* modENCODE. *Science* 330:1787–1797.
8. Gerstein MB, et al. (2010) Integrative analysis of the *Caenorhabditis elegans* genome by the modENCODE project. *Science* 330:1775–1787.
9. Lee S, et al. (2011) Accurate quantification of transcriptome from RNA-Seq data by effective length normalization. *Nucleic Acids Res* 39:e9.
10. Mortazavi A, Williams BA, McCue K, Schaeffer L, Wold B (2008) Mapping and quantifying mammalian transcriptomes by RNA-Seq. *Nat Methods* 5:621–628.
11. Feng J, et al. (2010) Inference of isoforms from short sequence reads. *14th Annual International Conference on Research in Computational Molecular Biology (RECOMB 2010)*, Lecture Notes on Computer Science, 6044 (Springer, Berlin/Heidelberg), pp 138–157.
12. Jiang H, Wong WH (2009) Statistical inferences for isoform expression in RNA-Seq. *Bioinformatics* 25:1026–1032.
13. Li B, Ruotti V, Stewart RM, Thomson JA, Dewey CN (2010) RNA-Seq gene expression estimation with read mapping uncertainty. *Bioinformatics* 26:493–500.
14. Richard H, et al. (2011) Prediction of alternative isoforms from exon expression levels in RNA-Seq experiments. *Nucleic Acids Res* 38:e112.
15. Li W, Feng J, Jiang T (2011) IsoLasso: A LASSO regression approach to RNA-Seq based transcriptome assembly. *15th Annual International Conference on Research*

**Table 3.**  $\lambda^{(n)}$  selection results for different datasets

$n$	3	4	5	6	7	8	9	10
Datasets 1–2 (37 bp)	0.3	0.3	0.3	0.4	0.4	0.4	0.4	0.5
Datasets 3–4 (76 bp)	0.2	0.2	0.2	0.4	0.3	0.4	0.3	0.3
Simulation data (37 bp)	0.3	0.3	0.3	0.4	0.4	0.4	0.4	0.5
16 candidate $\lambda$ s: $10^{-6}$ , $10^{-4}$ , $10^{-3}$ , 0.01, 0.04, 0.07, 0.1, 0.2, 0.3, 0.4, 0.5, 0.6, 0.7, 0.8, 0.9, 1								

note that this is a variant of Lasso, a regularization regression method for cases in which the number of parameters to be estimated exceeds the number of observations and most of the parameters are expected to be zeros (22). The difference between our penalty term and the one in standard Lasso is that the latter only aims to limit the number of discovered isoforms without favoring longer ones. Discussions about choosing  $L_1$  over  $L_0$  regularization and using different likelihoods in the linear model are in *SI Text*.

The selection of the regularization parameter  $\lambda$  (Eq. 4) is by a stability criterion that aims to return the most stable results over different runs of estimation (26). Because low signal-to-noise ratios in lowly expressed genes may significantly bias the  $\lambda$  selection and genes of the same number of subexons have similar  $\dim(\mathbf{p})$  and  $\dim(\mathbf{b})$  in Eq. 4, we group genes by their numbers of subexons  $n$  and select an optimal  $\lambda^{(n)}$  for each group from 16 candidate values  $(\lambda_i)_{i=1}^{16}$  (see Table 3). The selection procedure is described in *SI Text*, and the chosen  $\lambda^{(n)}$  values for datasets 1–4 and the simulation data are in Table 3.

R package "penalized" (27) is used in the implementation.

**mRNA Isoform Abundance Estimation.** The SLIDE linear model (Eq. 3) can also be used for abundance estimation of discovered or other specified (e.g., annotated) isoform proportions. Because the number of discovered or annotated isoforms is smaller than the number of bin proportions, the linear model is identifiable. Thus, we use nonnegative least squares without a penalty term to estimate the isoform proportions. R package "NNLS" is used in the implementation (28).

**ACKNOWLEDGMENTS.** We thank Qunhua Li and Nathan Boley in Department of Statistics, University of California, Berkeley, for their insightful comments during discussions. This work is supported in part by Grants HG004695, HG005639, and EY019094 from the National Institutes of Health. We would like to thank the Statistical and Applied Mathematical Sciences Institute for providing great research environments to C.-R.J. to continue participating in this project.

in *Computational Molecular Biology (RECOMB 2011)*, Lecture Notes on Computer Science, 6577 (Springer, Berlin/Heidelberg), pp 168–188.

16. Flicek P, et al. (2011) Ensembl 2011. *Nucleic Acids Res* 39(Suppl 1):D800–D806.
17. Fujita PA (2011) The UCSC Genome Browser database: Update 2011. *Nucleic Acids Res* 39(Suppl 1):D876–D882.
18. Frohman MA, Dush MK, Martin GR (1988) Rapid production of full-length cDNAs from rare transcripts: Amplification using a single gene-specific oligonucleotide primer. *Proc Natl Acad Sci USA* 85:8998–9002.
19. Shiraki T, et al. (2003) Cap analysis gene expression for high-throughput analysis of transcriptional starting point and identification of promoter usage. *Proc Natl Acad Sci USA* 100:15776–15781.
20. Guttman M, et al. (2010) Ab initio reconstruction of cell typespecific transcriptomes in mouse reveals the conserved multi-exonic structure of lincRNAs. *Nat Biotechnol* 28:503–510.
21. Adams MD, et al. (2003) Complementary DNA sequencing: Expressed sequence tags and human genome project. *Science* 252:1651–1656.
22. Tibshirani R (1996) Regression shrinkage and selection via the lasso. *J R Stat Soc Series B Stat Methodol* 58:267–288.
23. Liu S, Lin L, Jiang P, Wang D, Xing Y (2011) A comparison of RNA-Seq and high-density exon array for detecting differential gene expression between closely related species. *Nucleic Acids Res* 39:578–588.
24. Xia Z, Wen J, Chang C, Zhou X (2011) NSMAP: A method for spliced isoforms identification and quantification from RNA-Seq. *BMC Bioinformatics* 12:162.
25. Meinshausen N, Bühlmann P (2010) Stability selection. *J R Stat Soc Series B Stat Methodol* 72:417–473.
26. Dahinden C, Parmigiani G, Emerick MC, Bühlmann P (2007) Penalized likelihood for sparse contingency tables with an application to full-length cDNA libraries. *BMC Bioinformatics* 8:1–11.
27. Goeman JJ (2010) Penalized: L1 (Lasso) and L2 (Ridge) penalized estimation in GLMs and in the Cox model. R package version 0.9-31., Available at <http://cran.r-project.org/web/packages/penalized/>.
28. Mullen KM, van Stokkum IHM (2010) nnls: The Lawson-Hanson algorithm for non-negative least squares (NNLS). R package version 1.3., Available at <http://cran.r-project.org/web/packages/nnls/>.